COMMUNICATION

CrossMark
click for updates

A significant enhancement of water vapour uptake at low pressure by amine-functionalization of UiO-67†

Nakeun Ko,[a] Jisu Hong,[a] Siyoung Sung,[a] Kyle E. Cordova,[b] Hye Jeong Park,*[a] Jin Kuk Yang*[a] and Jaheon Kim*[a]

The functionalization of UiO-67 with $-NH_2$ groups enhances CO_2 and CH_4 adsorption at 1 bar and 298 K and positively influences the framework's interaction with water as evidenced by the significant enhancement of water vapour adsorption at $0.1 < P/P_0 < 0.3$ and 298 K.

Metal–organic frameworks (MOFs) are composed of well-defined inorganic clusters and organic linkers, which afford various pore structures and the ability to functionalize the interior pore surfaces for enhanced gas storage and separation properties.[1–6] MOFs have recently attracted attention as potential water sorbents for adsorptive heat transformation processes used in thermally driven adsorption chillers (TDCs) or adsorption heat pumps.[7–9] In this process, a sorbent material, such as a MOF, adsorbs water causing a decrease in the temperature of the water reservoir, which is thus utilized as a coolant for TDCs. The adsorbed water is then desorbed at ~80 °C by waste heat to generate a recyclable heat transformation system.[8] For the efficient usage of waste heat, water sorbents are required to have as much water uptake as possible over a relative pressure range of $P/P_0 = 0.05–0.4$,[7,8] or more properly to have a steep increase in water uptake at $P/P_0 = 0.1–0.3$.[9] In this case, water sorbents exhibit sigmoidal isotherms within this pressure range, which maximizes thermal mass utilization. In order to fulfill this requirement, the interactions between the sorbent pore surfaces and water molecules must be adjusted properly.

It is important to note that although MOFs such as Al-fumarate,[8] CAU-10,[10] MOF-814[11] are constructed from hydrophobic organic linkers, these materials exhibit large water uptake at low relative pressure. Furthermore, the isotherm profiles of these MOFs display sigmoidal-shaped adsorption and desorption branches with little hystereses.[7] However, these MOFs are rare examples because their water adsorption and desorption mechanisms are not easily predictable based solely on their structures and composition.[7,12] As opposed to designing and synthesizing the desired MOFs directly, it may be a more worthwhile strategy to tune the water affinity properties of known MOF structures through chemical modification of their organic linkers. Accordingly, one such approach is to introduce hydrophilic $-NH_2$ groups to facilitate greater water adsorption at lower relative pressures. Indeed, this approach has proven to be successful in MIL-101-NH_2,[13,14] MIL-125-NH_2,[12] Ga-MIL-53-NH_2,[12] In-MIL-68-NH_2[12] and Zr-UiO-66-NH_2.[12,15] Herein, we report the effect of incorporating $-NH_2$ functionalities on the water adsorption behavior of UiO-67, formulated as $Zr_6O_4(OH)_4(BPDC)_6$ (BPDC = 4,4′-biphenyl-dicarboxylate). UiO-67 is an isoreticularly expanded version of UiO-66, and due to its increased pore sizes,[16,17] steep water uptake takes place at a higher relative pressure ($P/P_0 \sim 0.4$) than that of UiO-66 ($P/P_0 \sim 0.2$).[18,19] Therefore, in order to achieve a higher water uptake over a lower pressure range, we have prepared UiO-67-$(NH_2)_2$, which has two $-NH_2$ groups incorporated on the BPDC linker.[20,21]

UiO-67 and its derivatives have been prepared by employing one of the five different solvothermal reactions that use *N,N*-dimethylformamide (DMF) as the main solvent: (a) $ZrCl_4$ with the corresponding BPDC linker,[15–17,21–23] (b) a Zr methacrylate oxo cluster precursor with a BPDC linker,[24] (c) $ZrCl_4$ with a BPDC linker and a modulator (benzoic acid or acetic acid),[25] (d) $ZrOCl_2$ with a BPDC linker and a modulator (formic acid),[11] and (e) $ZrCl_4$ with a BPDC linker and HCl.[20] While method (b) is a modular approach that utilizes a Zr-complex molecule as a precursor (or "module"), the methods (c) and (d) appear to produce 'Zr-cluster modules' *in situ* with the modulators being replaced by linkers to form extended structures,

[a]Institute for Integrative Basic Sciences and Department of Chemistry, Soongsil University, Seoul 156-743, Korea. E-mail: parkhyejeong83@gmail.com, jinkukyang@ssu.ac.kr, jaheon@ssu.ac.kr; Fax: +82 2 824 4383; Tel: +82 2 820 0459
[b]Center for Molecular and NanoArchitecture, Vietnam National University – Ho Chi Minh City, 721337, Vietnam

which is akin to ligand exchange observed in molecular complexes.[26] Method (e) provides crystalline UiO MOFs, albeit with some missing linkers that lead to increased surface areas. However, due to the very short reaction time, this method is only useful for scale-up purposes.

In this report, we have chosen method (c) for obtaining crystalline products of UiO-67 and UiO-67-$(NH_2)_2$. In general, the procedure is such that a DMF solution of $ZrCl_4$, 4,4′-biphenyl-dicarboxylic acid (H_2BPDC) or 2,2′-diaminobiphenyl-4,4′-dicarboxylic acid (H_2BPDC-$(NH_2)_2$), and a large amount of benzoic acid (molar ratio of linker : benzoic acid = 1 : 30 and 1 : 40 for UiO-67 and UiO-67-$(NH_2)_2$, respectively) were heated at 120 °C for 2 days to give each product (Section S2 in ESI†). To remove any remaining unreacted species, the obtained crystalline materials were washed thoroughly with DMF and acetone.

The chemical compositions of UiO-67 and UiO-67-$(NH_2)_2$ were determined by elemental analysis (EA) and ^{1}H-NMR measurements using the washed samples that were subsequently activated (removal of guest species within the pores) at 150 °C for 12 h under vacuum. A previous report had suggested that benzoic acid is entrapped within the UiO-67 structure and, consequently, cannot be completely removed during the washing process.[25] In our case, the ^{1}H-NMR spectrum for a digested UiO-67 sample ($NaOD/D_2O$) displayed similar signals corresponding to benzoate or formate. Although formate was not used in the initial synthesis, this molecule was produced due to the decomposition of DMF during the solvothermal reaction. It is unlikely that the small modulators observed in the NMR spectra are a result of entrapment within the pores, especially after thoroughly washing the materials with polar solvents. In contrast, we presume that these molecules take part in the Zr-cluster assemblies similar to some Zr-MOFs where the modulators (formates) were identified in the crystal structures.[11] Based on the integration of the signals, including the BPDCs, the chemical formula of UiO-67 was estimated to be $Zr_6O_4(OH)_4(BPDC)_{5.1}(benzoate)_{1.2}$ $(formate)_{0.6}$, which was in good agreement with the results obtained from EA. Similarly, the ^{1}H-NMR analysis for a digested sample of UiO-67-$(NH_2)_2$ afforded a chemical formula of $Zr_6O_4(OH)_4(BPDC$-$(NH_2)_2)_{4.1}(benzoate)_{0.6}(formate)_{3.2}$. The EA results for UiO-67-$(NH_2)_2$ corresponded well with this finding when 7 water molecules were additionally considered – it appears as though the evacuated sample adsorbed moisture from the air before the EA measurement was carried out. It is noteworthy that the digestion of UiO-67-$(NH_2)_2$ with HF produced many unidentified proton signals, presumably due to side reactions involving HF (Fig. S7†).[21] As the BPDC-$(NH_2)_2$ linker alone did not react with HF in our control experiments, it is believed that Zr ions play an important role in mediating the degradation of the organic linker.

The crystal structure of UiO-67 was determined using single crystal X-ray diffraction (SCXRD) analysis (Section S4 in ESI†).[27] The main features of this structure are almost the same as those proposed by other physical analyses, including an X-ray diffraction (PXRD) method.[16,17,23] In the crystal struc-
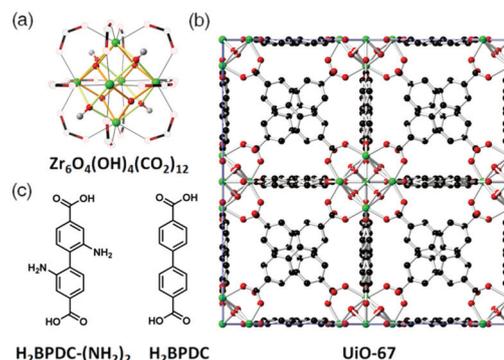

Fig. 1 (a) An inorganic secondary building unit of UiO-67. (b) The crystal structure of UiO-67. (c) Linear linker (H_2BPDC) for the preparation of UiO-67 and its amine-functionalized form (H_2BPDC-$(NH_2)_2$) for UiO-67-$(NH_2)_2$. In (a), Zr ions and hydroxo H atoms are displayed as green and grey balls, respectively. C and O atoms are depicted as black and red balls, respectively.

ture of UiO-67, similar to what has been observed in other Zr-MOFs[11,28] and molecular Zr-based complexes,[26] the oxo (μ_3-O) and hydroxo (μ_3-OH) oxygen atoms were clearly distinguished (Fig. 1, Fig. S5†). However, for UiO-67-$(NH_2)_2$, the obtained crystals were too small to be analyzed by SCXRD. Therefore, the structure of UiO-67-$(NH_2)_2$ was corroborated through PXRD data. The measured PXRD patterns of both UiO-67 and UiO-67-$(NH_2)_2$ coincided with the simulated pattern generated from the crystal structure of UiO-67, indicating that both frameworks are isostructural to one another (Fig. 2). The broad peaks observed in the PXRD pattern of UiO-67-$(NH_2)_2$ suggest that the crystallinity of this material was not as good as that of UiO-67. Thermogravimetric analysis (TGA) measurements in air indicated that UiO-67 was more stable than UiO-67-$(NH_2)_2$; UiO-67 and UiO-67-$(NH_2)_2$ started to decompose at *ca.* 400 and 300 °C, respectively (Section S6 in ESI†). TGA curves for each of the free linkers (H_2BPDC or H_2BPDC-$(NH_2)_2$) were also measured. It was found that the BPDC linker in UiO-67 was thermally more stable than that of the free H_2BPDC
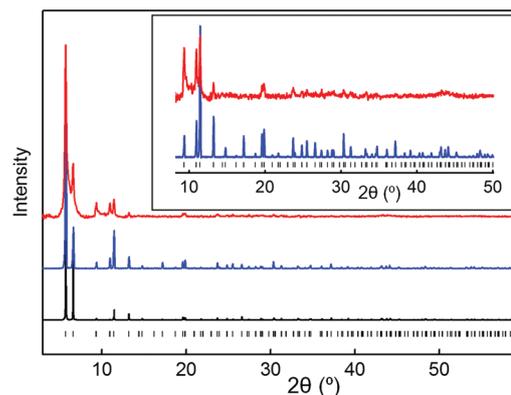

Fig. 2 The PXRD patterns of UiO-67 (blue) and UiO-67-$(NH_2)_2$ (red) are compared to a simulated pattern (black) generated from the crystal structure of UiO-67. The inset shows a magnified region of the patterns. Fig. S3† shows these patterns in a full 2θ range.

(Section S6†). In contrast, the BPDC-$(NH_2)_2$ linker in UiO-67-$(NH_2)_2$ decomposed more readily than the free H_2BPDC-$(NH_2)_2$ at a slightly lower temperature. The occluded guest molecules were mostly removed at 120 °C for UiO-67 and at 170 °C for UiO-67-NH_2, indicating that the amino groups in UiO-67-NH_2 might hinder the facile removal of these guest molecules.

The permanent porosity of UiO-67 and UiO-67-$(NH_2)_2$ was established by N_2 adsorption isotherms carried out at 77 K (Fig. S12†). The corresponding Brunauer–Emmett–Teller (BET) surface areas of UiO-67 and UiO-67-$(NH_2)_2$ were calculated to be 2300 and 1360 m^2 g^{-1}, respectively. The solvent-accessible surface areas, calculated by using ordered structural models, were determined to be 2920 and 2530 m^2 g^{-1} for UiO-67 and UiO-67-$(NH_2)_2$, respectively (Section S8 in ESI†). The BET surface area of UiO-67 is comparable to or larger than other reported values: 1441,[21] 1877,[23] 2145,[19] 2400,[25] 2500,[20] and 3000[25] m^2 g^{-1}. In contrast, the measured BET surface area of UiO-67-$(NH_2)_2$ (59% of the BET surface area of UiO-67) is much less than expected (87% of the solvent-accessible surface area of UiO-67). This is presumably due to the poor crystallinity observed for the prepared sample. Nevertheless, the CO_2 and CH_4 adsorption measurements conducted at 254, 273, and 298 K and under 1 bar indicated that at all measurement temperatures, UiO-67-$(NH_2)_2$ displayed a greater gas uptake than UiO-67 (Fig. 3). Furthermore, the calculated gas adsorp-

tion enthalpies were 14.6 (CH_4) and 23.4 (CO_2) kJ mol^{-1} for UiO-67, and 16.7 (CH_4) and 25.5 (CO_2) kJ mol^{-1} for UiO-67-$(NH_2)_2$ (Section S7 in ESI†). The increase in gas uptake (both CO_2 and CH_4) as well as heat of adsorption support the fact that the –NH_2 groups play a crucial role in enhancing the interactions between the framework surfaces and gas molecules.

The water vapour adsorption isotherms for UiO-67 and UiO-67-$(NH_2)_2$ were measured at 298 K (Fig. 4) and their uptake capacities at P/P_0 = 0.1, 0.3 and 0.9 were compared with one another (Table 1). As shown in Fig. 4, UiO-67 adsorbed very little water until P/P_0 = 0.5, after which it exhibited a steep uptake until P/P_0 = 0.6. Furthermore, the uptake capacity then hardly increased after P/P_0 = 0.6, which led to a calculated total uptake capacity of 293 mg g^{-1} (22.7 wt%) at P/P_0 = 0.9. The overall profile of the adsorption isotherm shows a sigmoidal shape with a vertical adsorption isotherm in the range of P/P_0 = 0.5–0.6. In contrast to the water adsorption behaviour of UiO-67, the water vapour isotherm for UiO-67-$(NH_2)_2$ demonstrated an initial water uptake close to P/P_0 = 0, which then gave way to an abrupt increase at P/P_0 = 0.2. This clearly indicates the MOF's strong affinity toward water, which is a result of the added –NH_2 functionalities within the pores. The resulting water uptake capacity of UiO-67-$(NH_2)_2$ increased significantly in the optimal pressure range of P/P_0 = 0.1–0.3 when compared to UiO-67. Indeed, the capacity in this relative pressure range calculated for UiO-67 and UiO-67-$(NH_2)_2$ was
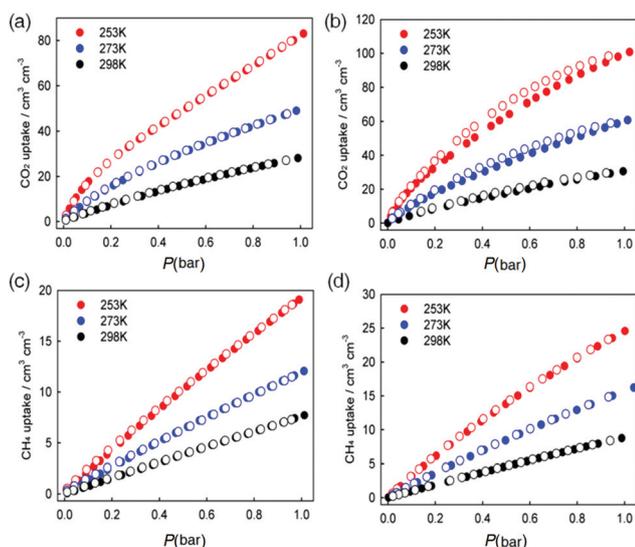

Fig. 3 CO_2 adsorption isotherms of (a) UiO-67 and (b) UiO-67-$(NH_2)_2$, and CH_4 adsorption isotherms of (c) UiO-67 and (d) UiO-67-$(NH_2)_2$ are represented with filled (adsorption) and open (desorption) marks.
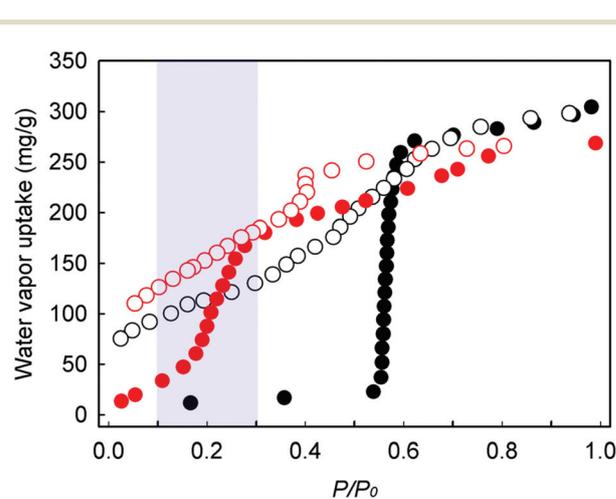

Fig. 4 Water vapour adsorption isotherms of UiO-67 (black) and UiO-67-$(NH_2)_2$ (red) measured at 298 K. The optimal P/P_0 range (P/P_0 = 0.1–0.3) is highlighted with a blue block: P_0: 3.169 kPa. The adsorption and desorption branches are represented by filled and open circles, respectively.

Table 1 Porosity and water vapour adsorption properties of UiO-67 and UiO-67-$(NH_2)_2$

	Surface area (m^2 g^{-1})		Pore volume (cm^3 g^{-1})	Water uptake (mg g^{-1}) (wt%)		
MOF	BET	Langmuir		P/P_0 = 0.1	P/P_0 = 0.3	P/P_0 = 0.9
UiO-67	2300	2730	0.99	8 (0.8)	15 (1.5)	293 (22.7)
UiO-67-$(NH_2)_2$	1360	1780	0.64	30 (2.9)	173 (14.7)	262 (20.8)

found to be 0.7 and 11.8 wt%, respectively. After this abrupt increase situated around $P/P_0 = 0.2$, the water uptake capacity for UiO-67-$(NH_2)_2$ was 173 mg g^{-1} at $P/P_0 = 0.3$.

As most MOFs do not have high water stability,[7] a limited number of water-stable MOFs, based on Al, Cr, and/or Zr secondary building units, can be regarded as suitable water adsorbents.[7,8] Recently, it was reported that UiO-67 is not stable in water, which is in stark contrast to the impressive water and chemical stability exhibited by UiO-66.[19,29] The reasoning behind this lack of stability has been ascribed to the flexibility of the longer BPDC linker. This linker leads to the framework being more susceptible to structural distortion due to the more pronounced capillary forces that occur during the water desorption processes. Our findings support this reasoning, as the adsorbed water was not fully desorbed when looking at relative pressures near $P/P_0 \sim 0$ (Fig. 4 and S21†). This observation led us to suspect that both MOFs decomposed over the course of the water sorption measurements. The measured PXRD patterns of the collected samples, after water sorption, showed very broad diffraction peaks, which indicated a loss in crystallinity and, thus, instability of UiO-67 and UiO-67-$(NH_2)_2$ in water (Fig. S4†). After the water sorption measurements, the collected materials were almost nonporous based on N_2 sorption measurements (Fig. S12†). Thus, the observed large hysteresis in the isotherms, shown in Fig. 4, is ascribed to framework decomposition involving ligand replacement with water molecules.[29]

In conclusion, the –NH_2 functionalization of UiO-67 was very effective in shifting the sigmoidal water vapour adsorption curve down to lower relative pressures and positioning the steepest uptake region at $P/P_0 = 0.1$–0.3. Although UiO-67-$(NH_2)_2$ was degraded after the water sorption measurement, this work indicates that the water adsorption properties of MOFs can be fine-tuned through amine-functionalization of framework surfaces in medium-sized pore (ca. 2 nm) walls.

Acknowledgements

Notes and references

1 Y. Yan, S. Yang, A. J. Blake and M. Schröder, *Acc. Chem. Res.*, 2014, **47**, 296.

2 M. P. Suh, H. J. Park, T. K. Prasad and D.-W. Lim, *Chem. Rev.*, 2012, **112**, 782.

3 J.-R. Li, J. Sculley and H.-C. Zhou, *Chem. Rev.*, 2012, **112**, 869.

4 K. Sumida, D. L. Rogow, J. A. Mason, T. M. McDonald, E. D. Bloch, Z. R. Herm, T.-H. Bae and J. R. Long, *Chem. Rev.*, 2012, **112**, 724.

5 J. A. Mason, M. Veenstrab and J. R. Long, *Chem. Sci.*, 2014, **5**, 32.

6 Y. He, W. Zhou, G. Qiand and B. Chen, *Chem. Soc. Rev.*, 2014, **43**, 5657.

7 J. Canivet, A. Fateeva, Y. Guo, B. Coasne and D. Farrusseng, *Chem. Soc. Rev.*, 2014, **43**, 5594.

8 F. Jeremias, D. Frohlich, C. Janiak and S. K. Henninger, *New J. Chem.*, 2014, **38**, 1846.

9 Y. I. Aristov, *Appl. Therm. Eng.*, 2013, **50**, 1610.

10 H. Reinsch, M. A. van der Veen, B. Gil, B. Marszalek, T. Verbiest, D. de Vos and N. Stock, *Chem. Mater.*, 2013, **25**, 17.

11 H. Furukawa, F. Gándara, Y.-B. Zhang, J. Jiang, W. L. Queen, M. R. Hudson and O. M. Yaghi, *J. Am. Chem. Soc.*, 2014, **136**, 4369.

12 J. Canivet, J. Bonnefoy, C. Daniel, A. Legrand, B. Coasne and D. Farrusseng, *New J. Chem.*, 2014, **38**, 3102.

13 G. Akiyama, R. Matsuda, H. Sato, A. Hori, M. Takata and S. Kitagawa, *Microporous Mesoporous Mater.*, 2012, **157**, 89.

14 A. Khutia, H. U. Rammelberg, T. Schmidt, S. Henninger and C. Janiak, *Chem. Mater.*, 2013, **25**, 790.

15 G. E. Cmarik, M. Kim, S. M. Cohen and K. S. Walton, *Langmuir*, 2012, **28**, 15606.

16 J. H. Cavka, S. Jakobsen, U. Olsbye, N. Guillou, C. Lamberti, S. Bordiga and K. P. Lillerud, *J. Am. Chem. Soc.*, 2008, **130**, 13850.

17 Q. Yang, V. Guillerm, F. Ragon, A. D. Wiersum, P. L. Llewellyn, C. Zhong, T. Devic, C. Serrec and G. Maurin, *Chem. Commun.*, 2012, **48**, 9831.

18 F. Jeremias, V. Lozan, S. K. Henninger and C. Janiak, *Dalton Trans.*, 2013, **42**, 15967.

19 J. B. DeCoste, G. W. Peterson, H. Jasuja, T. G. Glover, Y. Huang and K. S. Walton, *J. Mater. Chem. A*, 2013, **1**, 5642.

20 M. J. Katz, Z. J. Brown, Y. J. Colón, P. W. Siu, K. A. Scheidt, R. Q. Snurr, J. T. Hupp and O. K. Farha, *Chem. Commun.*, 2013, **49**, 9449.

21 S. J. Garibay, Dissertation, UC San Diego, 2011.

22 S. J. Garibay and S. M. Cohen, *Chem. Commun.*, 2010, **46**, 7700.

23 S. Chavan, J. G. Vitillo, D. Gianolio, O. Zavorotynska, B. Civalleri, S. Jakobsen, M. H. Nilsen, L. Valenzano, C. Lamberti, K. P. Lillerud and S. Bordiga, *Phys. Chem. Chem. Phys.*, 2012, **14**, 1614.

24 V. Guillerm, S. Gross, C. Serre, T. Devic, M. Bauer and G. Férey, *Chem. Commun.*, 2010, **46**, 767.

25 A. Schaate, P. Roy, A. Godt, J. Lippke, F. Waltz, M. Wiebcke and P. Behrens, *Chem. – Eur. J.*, 2011, **17**, 6643.

26 M. Puchberger, F. R. Kogler, M. Jupa, S. Gross, H. Fric, G. Kickelbick and U. Schubert, *Eur. J. Inorg. Chem.*, 2006, 3283.

27 The structural model of UiO-67 was refined without the modulators for simplicity.

28 L. Valenzano, B. Civalleri, S. Chavan, S. Bordiga, M. H. Nilsen, S. Jakobsen, K. P. Lillerud and C. Lamberti, *Chem. Mater.*, 2011, **23**, 1700.

29 J. E. Mondloch, M. J. Katz, N. Planas, D. Semrouni, L. Gagliardi, J. T. Hupp and O. K. Farha, *Chem. Commun.*, 2014, **50**, 8944.